



## Experimental and theoretical study of new Schiff bases based on imidazo(1,2-a)pyridine as corrosion inhibitor of mild steel in 1M HCl



Abdelmalik EL AATIAOUI<sup>a,\*</sup>, Mohammed KOUDAD<sup>a</sup>, Tarik CHELFI<sup>b,\*</sup>, Sultan ERKAN<sup>c</sup>, Mohamed AZZOUZI<sup>b</sup>, Abdelouahad AOUNITI<sup>b</sup>, Kaya SAVAŞ<sup>c</sup>, Mohammed KADDOURI<sup>b</sup>, Noureddine BENCHAT<sup>b</sup>, Adyl OUSSAID<sup>a</sup>

<sup>a</sup> Laboratory of Molecular Chemistry, Materials and Environment (LCM2E), Faculty Multidisciplinary of Nador, University Mohammed the first, BP 524, Oujda 60000, Morocco

<sup>b</sup> Laboratory of Applied Chemistry and Environment, Faculty of Science, University Mohammed the first, BP 524, Oujda 60000, Morocco

<sup>c</sup> Faculty of Science, Department of Chemistry, Cumhuriyet University, Sivas 58140, Turkey

### ARTICLE INFO

#### Article history:

Received 13 August 2020

Revised 29 September 2020

Accepted 29 September 2020

Available online 30 September 2020

#### Keywords:

Imidazo(1,2-a)pyridine

Mild steel

HCl

Corrosion inhibition

Weight loss measurement

Electrochemical impedance spectroscopy (EIS)

DFT method

### ABSTRACT

In this work, we report a study on the synthesis and characterization, using several spectroscopic techniques such as IR, <sup>13</sup>C NMR, <sup>1</sup>H NMR and mass spectroscopy, of a new series of Schiff bases based on imidazo(1,2a)pyridine (IMP) scaffold, and the evaluation of their ability to inhibit the corrosion of mild steel in 1M HCl by mass loss techniques, Potentiodynamic polarization, electrochemical impedance spectroscopy (EIS), and quantum chemistry calculation based on density functional theory (DFT).

The obtained results show that these inhibitors, namely (E)-N-(2-phenylimidazo(1,2-a)pyridin-3-yl)-1-(1H-pyrrol-2-yl)methanimine (IMP<sub>1</sub>), (E)-N-(2-phenylimidazo(1,2-a)pyridin-3-yl)-1-(thiophen-2-yl)methanimine (IMP<sub>2</sub>) and (E)-1-(5-nitrothiophen-2-yl)-N-(2-phenylimidazo(1,2-a)pyridin-3-yl)methanimine (IMP<sub>3</sub>), act only by reducing the cathode area without changing the mechanism of the cathodic reaction, and that the effectiveness of the inhibition increases with increasing concentration of the inhibitors. The adsorption of the studied compounds on the surface of mild steel follows the Langmuir isotherm model. And finally, we highlighted the existence of a correlation between the molecular structure of the tested inhibitors and their anticorrosion activity.

© 2020 Elsevier B.V. All rights reserved.

## 1. Introduction

Imidazo[1,2-a]pyridines, and particularly their Schiff bases, are a very important class of heterocycles which have received particular interest in the chemical [1–5] and pharmaceutical fields [6–8]. They are described, as well as their syntheses in numerous works and studies [9,10].

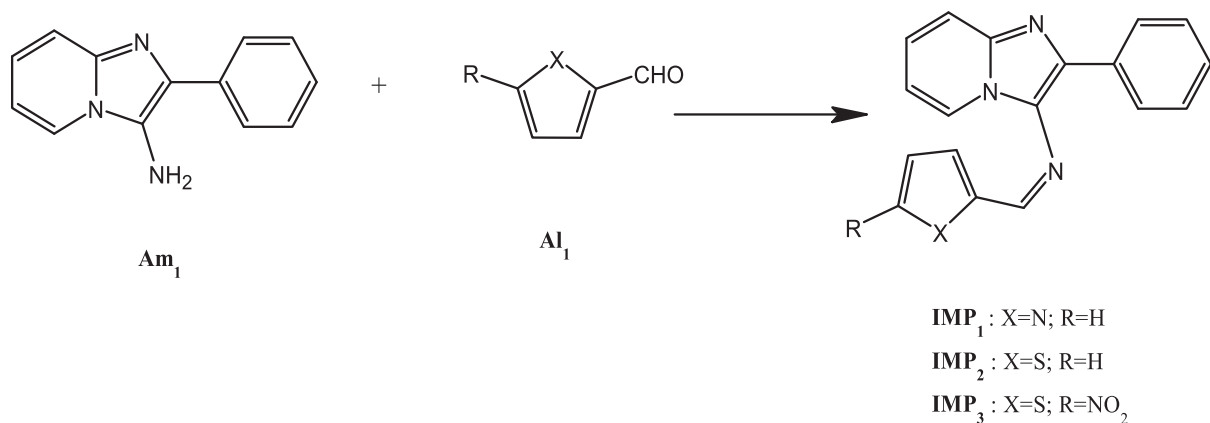
The use of organic compounds, and in particular Schiff bases, have been studied recently as a corrosion inhibitors for various metals and alloys in acidic medium [11–19], many of which have

been reported as a potential corrosion inhibitors for mild steel [11,20–23]. These compounds, in general, are adsorbed on the surface of the metal by blocking active corrosion sites. Some reported researches [14,24,25] show that the effectiveness of Schiff base inhibition is much higher than that of aldehydes and corresponding amines, and this may be due to the presence of the imine group –C=N– in those molecules.

Quantum chemical calculations have been widely used to model the mechanism of interaction between the corrosion inhibitor and the metal surface and target the active inhibitor sites used. Thus, it has been reported that the inhibition efficiency of corrosion depends on the physico-chemical and electronic properties of organic inhibitors, as well as on the interaction between the inhibitor and the metal surface. These theoretical studies provide

\* Corresponding authors.

E-mail addresses: [a.elatiaoui@ump.ma](mailto:a.elatiaoui@ump.ma) (A.E. AATIAOUI), [tchelfi@sante.gov.ma](mailto:tchelfi@sante.gov.ma) (T. CHELFI).



**Scheme 1.** Synthetic route for preparation of Schiff bases  $\text{IMP}_{1-3}$ .

access to several quantum parameters of organic entities, namely frontiers molecular orbitals and charges which are widely used to assess the reactivity of molecules [12,26–29].

In continuation to our previous work, we have synthesized new aromatic Schiff bases  $\text{IMP}_{1-3}$  (Scheme 1) using a condensation process between 2-phenylimidazo(1,2-a)pyridine-3-amine and three different aromatic aldehydes. The main objective of the present study was to investigate their ability to inhibit corrosion of mild steel in corrosive medium such as 1M hydrochloric acid at 25 °C, using some electrochemical techniques especially weight loss measurement (WLM), Potentiodynamic polarization, and electrochemical impedance spectroscopy (EIS).

Besides, we aimed at determining the relationships between physicochemical, electronic properties and inhibition efficiency, and then target the active binding sites of these Schiff bases through density functional theory (DFT) quantum chemical calculations.

## 2. Experimental details

### 2.1. Materials, solutions and instrumentations

All the chemicals used in this study were purchased from Sigma-Aldrich and they were used without further purification. All tests on Kofler bench, Infrared (IR), Nuclear magnetic resonance (NMR) and the Elemental composition are conducted according to international standards.

The NMR spectra were recorded on a Bruker AVANCE 300 ( $^1\text{H}$ ,  $^{13}\text{C}$ ). The chemical shifts are expressed in ppm relative to the Tetramethylsilane (TMS) used as a reference ( $\delta_{\text{TMS}} = 0$ ). The solvent used is  $\text{CDCl}_3$ . The following symbols have been used: s = singlet; ls = large singlet; d = doublet; dd = doubled doublet; t = triplet; q = quadruple; m = multiplet and the coupling constants J are expressed in Hz. The FT-IR spectra were recorded on SHIMADZU 8400s instrument by using KBr plates in the range 4000–500  $\text{cm}^{-1}$ . The absorption frequencies are expressed in  $\text{cm}^{-1}$ . The mass spectra were obtained with an API 3200 LC/MS Mass Spectrometer.

The corrosive solutions of 1.0 M HCl were prepared by dilution of an analytical grade 37% HCl with bi-distilled water. The concentration range of green inhibitor employed was  $10^{-3}$ – $10^{-5}$  (M).

Coupons were cut into  $2 \times 2 \times 0.05$  cm dimensions having composition (0.09%P, 0.01% Al, 0.38% Si, 0.05% Mn, 0.21% C, 0.05% S and the rest of the iron.

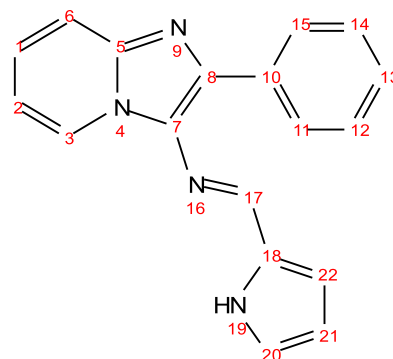
### 2.2. Chemistry

#### 2.2.1. Schiff bases of imidazo(1,2-a)pyridine $\text{IMP}_{1-3}$ synthesis

The synthesis of the studied imidazo(1,2-a)pyridines  $\text{IMP}_{1-3}$  was carried out following the synthetic route shown in Scheme 1. Two drops of acetic acid as catalyst (0.3 mL) were added to (2.39 mmol) of 2-phenylimidazo[1,2-a]pyridin-3-amine ( $\text{Am}_1$ ) dissolved in the minimum of diethyl ether (20 mL) and stirred for 30 minutes at room temperature. Then, (2.39 mmol) of substituted aldehydes ( $\text{Al}_{1-3}$ ) have been added to the mixture and left under stirring for 24 h until the aldehyde is completely consumed (The progress of the reaction has been monitored by thin layer chromatography TLC). Once the aldehyde has been completely consumed, the product formed was filtered and washed with dry ether.

The molecular structures and the spectroscopic identifications for the synthesized IMP are listed below [30].

#### 2.2.2. (E)-N-(2-phenylimidazo[1,2-a]pyridin-3-yl)-1-(1H-pyrrol-2-yl)methanimine ( $\text{IMP}_1$ )



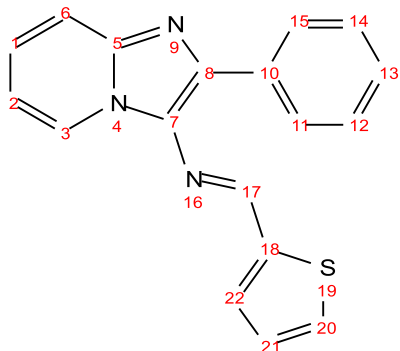
Green powder. Yield 89,80%. Mp: 178–180 °C.  $R_f = 0.55$  (silica,  $\text{CH}_2\text{Cl}_2/\text{CH}_3\text{OH} : 9/1$ ).  $^1\text{H NMR}$  (300 MHz,  $\text{CDCl}_3$ ,  $\delta$  (ppm)): 8.62 (s, 1H,  $\text{N}_{19}\text{H}$ ); 8.48 (s, 1H,  $\text{N}=\text{C}_{17}\text{H}$ ); 8.23 (d, 1H,  $\text{C}_3\text{H}$ ,  $J = 6.9$  Hz); 7.83 (d, 2H,  $\text{C}_{12}\text{H}$   $\text{C}_{15}\text{H}$ ,  $J = 7.2$  Hz); 7.56 (d, 1H,  $\text{C}_6\text{H}$ ,  $J = 9$  Hz); 7.41 (t, 2H,  $\text{C}_{12}\text{H}$   $\text{C}_{14}\text{H}$ ,  $J = 12$  Hz); 7.30 (dd, 1H,  $\text{C}_{13}\text{H}$ ,  $J = 14.7$  Hz); 7.15 (t, 1H,  $\text{C}_1\text{H}$ ,  $J = 16.8$  Hz); 7.05 (s, 1H,  $\text{C}_{20}\text{H}$ ); 6.79 (t, 1H,  $\text{C}_2\text{H}$ ,  $J = 13.5$  Hz); 6.54 (s, 1H,  $\text{C}_{22}\text{H}$ ); 6.32 (s, 1H,  $\text{C}_{21}\text{H}$ ).

$^{13}\text{C NMR}$  (75 MHz,  $\text{CDCl}_3$ )  $\delta$ (ppm): 149.02; 142.47; 134.85; 128.77; 128.18; 127.59; 124.33; 123.42; 122.84; 117.42; 116.80; 112.04; 110.99.

**MS** (m/z) (M+): 258.1.

**IR:**  $\nu(\text{cm}^{-1})$ : 2353; 1687; 1653; 1550.

2.2.3. (*E*)-*N*-(2-phenylimidazo[1,2-*a*]pyridin-3-yl)-1-(thiophen-2-yl)methanimine (*IMP*<sub>2</sub>)

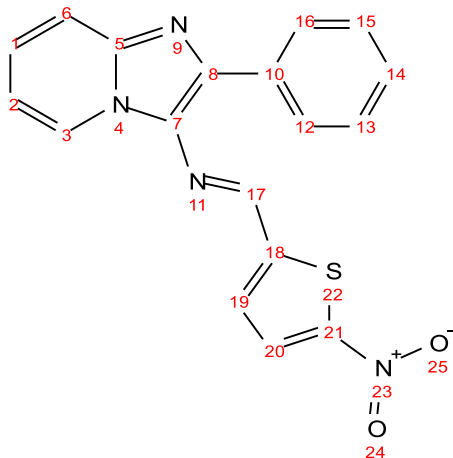


Yellow powder. Yield 86,15%. Mp: 125–127 °C. *R*<sub>f</sub> = 0.55 (silica, CH<sub>2</sub>Cl<sub>2</sub>/MeOH, 9/1).

<sup>1</sup>H NMR (300 MHz, DMSO, δ (ppm)): 9.22 (s, 1H, C<sub>17</sub>H=N); 8.61 (d, 1H, C<sub>3</sub>H, *J* = 6.24 Hz); 8.00 (d, 2H, C<sub>11</sub>H, C<sub>15</sub>H *J* = 7.26 Hz); 7.90 (d, 1H, C<sub>6</sub>H, *J* = 4.95); 7.49 (t, 8H, C<sub>1</sub>H, C<sub>2</sub>H, C<sub>12</sub>H, C<sub>13</sub>H, C<sub>14</sub>H, C<sub>20</sub>H, C<sub>21</sub>H, C<sub>22</sub>H).

MS (m/z) (M+1): 304. IR (KBr): ν (CH=N, imine) = 1605 cm<sup>-1</sup>.

2.2.4. (*E*)-1-(5-nitrothiophen-2-yl)-*N*-(2-phenylimidazo[1,2-*a*]pyridin-3-yl)methanimine (*IMP*<sub>3</sub>)



Brun powder. Yield 92,10%. Mp: 209–210 °C. *R*<sub>f</sub>: 0.6 (silica, CH<sub>2</sub>Cl<sub>2</sub>/CH<sub>3</sub>OH: 9/1).

<sup>1</sup>H NMR (300 MHz, CDCl<sub>3</sub>, δ (ppm)): 8.73 (s, 1H, N=C<sub>18</sub>H); 8.47 (d, 1H, C<sub>3</sub>H, *J* = 6.6 Hz); 7.83 (d, 1H, C<sub>20</sub>H, *J* = 4.2 Hz); 7.70 (d, 2H, C<sub>12</sub>H, C<sub>16</sub>, *J* = 6.9 Hz); 7.59 (d, 1H, C<sub>19</sub>H, *J* = 7.2 Hz); 7.46 (m, 3H, C<sub>13</sub>H, C<sub>14</sub>H, C<sub>15</sub>H); 7.32 (m, 1H, C<sub>6</sub>H, *J* = 15.9 Hz); 7.06 (d, 1H, C<sub>1</sub>H, *J* = 4.2 Hz) 6.98 (t, 1H; C<sub>2</sub>H, *J* = 13.5 Hz).

<sup>13</sup>C NMR (75 MHz, CDCl<sub>3</sub>) δ(ppm): 150.34; 144.23; 143.62; 143.56; 134.56; 129.07; 128.94; 128.63; 128.13; 126.73; 123.70; 117.63; 113.39.

IR ν (cm<sup>-1</sup>): 1655 cm<sup>-1</sup>, 1315 cm<sup>-1</sup>; 1232 cm<sup>-1</sup>.

MS (m/z) (M+1): 349.1.

## 2.3. Gravimetric measurements

### 2.3.1. Influence of inhibitor concentration

In this part of the study, we carried out gravimetric measurements on mild steel in 1M HCl medium in the absence and in the

presence of different concentrations of a series of compounds derived from **IMP**. The iron samples were exposed to the corrosive medium for a period of 6 h, at a temperature of 35 °C. The corrosion rate *W*<sub>corr</sub>(mg/h.cm<sup>2</sup>) is expressed according to the following relation:

$$W_{\text{corr}} = \frac{\Delta m}{S \cdot \Delta t} \quad (1)$$

The value of the inhibitory efficacy is the average of three tests carried out under the same conditions for each concentration. It is given by the following relation:

$$E\% = \frac{W_{\text{corr}} - W_{\text{corr}}(\text{inibi})}{W_{\text{corr}}} \times 100 \quad (2)$$

where *W*<sub>corr</sub> and *W*<sub>corr</sub>(inibi) are the corrosion rates of the sample, respectively, in the absence and in the presence of the inhibitor.

### 2.3.2. Adsorption isotherm

Determining the adsorption isotherms of inhibitors on the surface of steel is very important because they tell us about the nature of the metal-solution interaction. For this, we tested the experimental data with several isotherm of adsorption such as Langmuir, Temkin, and Frumkin isotherm [31].

## 2.4. Electrochemical measurement

### 2.4.1. Polarization measurements

The current intensity is measured between the working electrode and the platinum counter electrode and all potentials are referenced to the saturated calomel electrode. The latter is placed near the working electrode to minimize the influence of the ohmic drop. The potential applied to the sample varies continuously, with a scanning speed equal to 1 mV h<sup>-1</sup>, from -800 mV to -200 mV. The free potential of steel is stabilized after 30 min and measurements can then be made.

### 2.4.2. Electrochemical impedance spectroscopy

The electrochemical impedance diagrams for mild steel in 1M HCl in the presence of **IMP**<sub>1-3</sub>, at different concentrations are shown in the Fig. 5. To carry out these diagrams, we respected the same operating conditions as previously.

$$E_R\% = \frac{R_{\text{corr}}(\text{inh}) - R_{\text{corr}}}{R_{\text{corr}}(\text{inh})} \times 100 \quad (3)$$

$$C_{dl} = \frac{1}{2\pi f_{\text{max}} R_{tc}} \quad (4)$$

## 2.5. Temperature effect

The temperature of the corrosive medium is a factor which can modify the inhibitory efficiency of an inhibitor and the metal-inhibitor interaction, as it can also provide information on the mechanism of action of the inhibitor (chemisorption or physisorption) and on the activation energies of the corrosion process. Given the importance of this factor, we have carried out mass loss tests for steel in 1M HCl acid without and with the addition of inhibitors, in a temperature range between 35 and 65 °C. This for an immersion time of one hour and at a concentration of 10<sup>-3</sup>M, a concentration for which the inhibitory efficiency of inhibitor reaches the maximum value at temperature 35 °C. We chose the gravimetric method since it best reflects the phenomenon of corrosion as it is in the real state.

## 2.6. Quantum chemical calculations

The examined **IMP<sub>1-3</sub>** compounds were prepared with GaussView 5.0.8 [32] and the necessary calculations were made using Gaussian 09 Revision-D.01 and Gaussian 09 AML64L-Revision-D.01 [33]. All molecules are optimized using the DFT/B3LYP and M062X methods with 6-31G(d), 6-31++G(d), LANL2DZ and SDD [34] basis sets in gas phase.

Conceptual Density Functional Theory (**CDFT**) is a concept that offers simple equations in obtaining quantum chemical parameters. Some quantum chemical parameters such as the highest occupied molecular orbital energy (**E<sub>HOMO</sub>**), the lowest unoccupied molecular orbital energy (**E<sub>LUMO</sub>**), the energy gap (**ΔE**), hardness (**η**), softness (**σ**), electronegativity (**χ**), chemical potential (**μ**), global molecular electrophilicity (**ω**) index, global molecular nucleophilicity (**ε**) index, the electron accepting (**ω<sup>+</sup>**) and electron donating (**ω<sup>-</sup>**) powers, the number of transferred electrons (**ΔN**), and the electric dipole polarizability (**α**) are used to predict the corrosion inhibition activities of the chemical species studied approximately [35].

The equations of the parameters used based on the concept are as follows:

$$I = -E_{\text{HOMO}} \quad (5)$$

$$A = -E_{\text{LUMO}} \quad (6)$$

$$\eta = \frac{I - A}{2} \quad (7)$$

$$\sigma = \frac{1}{\eta} \quad (8)$$

$$\mu = -\chi = -\frac{I + A}{2} \quad (9)$$

$$\omega = \frac{\chi^2}{2\eta} \quad (10)$$

$$\varepsilon = \frac{1}{\omega} \quad (11)$$

$$\omega^+ = \frac{(I + 3A)^2}{16(I - A)} \quad (12)$$

$$\omega^- = \frac{(3I + A)^2}{16(I - A)} \quad (13)$$

$$\Delta N = \frac{\chi_{\text{Fe}} - \chi_{\text{inh}}}{2(\eta_{\text{Fe}} + \eta_{\text{inh}})} \quad (14)$$

$$\langle \alpha \rangle = \frac{1}{3} [\alpha_{xx} + \alpha_{yy} + \alpha_{zz}] \quad (15)$$

## 3. Results and discussions

### 3.1. Gravimetric measurement

#### 3.1.1. Influence of inhibitor concentration

Table 1 gives the values of the corrosion rate (W) and the percentage of the inhibitory efficiency (E%) calculated from gravimetric measurements for different concentrations of IMP in hydrochloric acid (1M) medium.

The analysis of these results shows that the synthetic ligands present a significant efficiency to inhibit the corrosion of mild steel in molar hydrochloric acid medium, as well as the increase in the concentration of the inhibitors leads to a decrease in the rate of corrosion, and on the other side a remarkable increasing in the inhibitory efficiency. The best inhibition rate is obtained in the pres-

**Table 1**

Weight loss data for mild steel 1M HCl without and with different concentrations of IMP<sub>1-3</sub> at 308 K.

Compounds	Concentration (M)	Corrosion rate (mg/cm <sup>2</sup> .h)	Efficiency (%)
Blank	1	0.827	-
IMP <sub>1</sub>	10 <sup>-3</sup>	0.0228	97
	5.10 <sup>-4</sup>	0.0315	96
	10 <sup>-4</sup>	0.2378	71
	5.10 <sup>-5</sup>	0.3242	60
	10 <sup>-5</sup>	0.3684	55
IMP <sub>2</sub>	10 <sup>-3</sup>	0.0416	94
	5.10 <sup>-4</sup>	0.089	89
	10 <sup>-4</sup>	0.1755	78
	5.10 <sup>-5</sup>	0.4534	45
	10 <sup>-5</sup>	0.5148	37
IMP <sub>3</sub>	10 <sup>-3</sup>	0.1121	86
	5.10 <sup>-4</sup>	0.1288	84
	10 <sup>-4</sup>	0.4274	48
	5.10 <sup>-5</sup>	0.5865	29
	10 <sup>-5</sup>	6.4909	21

**Table 2**

Thermodynamic parameters for the adsorption of IMP<sub>1</sub>, IMP<sub>2</sub> and IMP<sub>3</sub> in 1.0 M HCl on the carbon steel at 308K.

Compounds	Linear correlation	Slope	K	ΔG°(kJ mol <sup>-1</sup> )
IMP <sub>1</sub>	0.9988	1,0037	3,92.10 <sup>4</sup>	-37,371
IMP <sub>2</sub>	0.9979	1,0334	2,83.10 <sup>4</sup>	-35,538
IMP <sub>3</sub>	0.9929	1,0745	1,25.10 <sup>4</sup>	-34,443

ence of ligand IMP<sub>1</sub> (97%); It allows us to classify these compounds in the following order:

**IMP<sub>1</sub>** (97%) > **IMP<sub>2</sub>** (94%) > **IMP<sub>3</sub>** (86%)

#### 3.1.2. Adsorption isotherm

The corrosion inhibition efficiency effect of an organic molecule strongly depends upon its adsorption capability on a metal surface. Establishing a relationship between the adsorption process and inhibition behaviour is of crucial importance in studies of corrosion inhibition. An adsorption isotherm can explain the phenomenon which determines the retention or release of a substance from aqueous solution to the solid phase at a given temperature [36,37]. The results obtained experimentally have been applied to isotherms like Langmuir, Temkin and Freundlich where the Langmuir adsorption isotherm provided the best fit and can be described by the relation given below [36-39]:

- Temkin isotherm  $\exp(f.\theta) = K_{\text{ads}}.C$
- Freundlich isotherm  $\theta = K_{\text{ads}}.C$
- Langmuir isotherm  $(\theta/1-\theta) = K_{\text{ads}}.C$

where  $K_{\text{ads}}$  designates the equilibrium constant for adsorption process, C is the concentration of inhibitor and f is energetic inhomogeneities. The Langmuir equation can be rearranged as shown:

$$\frac{C}{\theta} = \frac{1}{K_{\text{ads}}} + C$$

In Fig. 1, we represent the calculated isotherm for the studied Schiff bases **IMP<sub>1-3</sub>**. The Analysis of this representation shows that the inhibitors **IMP<sub>1-3</sub>** are adsorbed on the metal surface according to the Langmuir model since the variation is linear and the regression coefficient is close to 1. These isotherms show that the adsorption of organic molecules on the metal surface is monolayer [40].

Also, from the Langmuir isotherm, we can have access to the values of the constant K and the adsorption energy  $\Delta G_{\text{ads}}^0$  which are listed in Table 2.

Generally, for  $\Delta G_{\text{ads}}$  values below than or equal to -20 kJ/mol the adsorption is due to physisorption electrostatic interaction between the charges at metal surface and inhibitor while for  $\Delta G_{\text{ads}}$

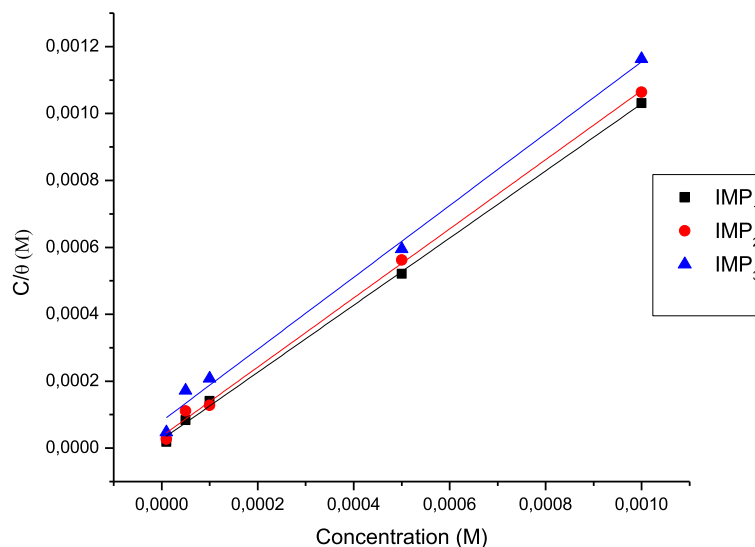


Fig. 1. Langmuir adsorption of  $IMP_{1-3}$  of the mild steel surface in 1 M HCl solution.

around  $-40$  kJ/mol, the adsorption is of chemisorption type, due to the formation of coordinate bonds by charge sharing or electron transfer from the neutral organic compound to the metal surface. Thus, from Table 2 the  $\Delta G_{ads}$  values for the studied inhibitors the adsorption for Schiff base derivatives  $IMP_{1-3}$  it is not typical chemisorption or physisorption but rather a combination of both (comprehensive adsorption) [41,42].

### 3.2. Electrochemical measurement

#### 3.2.1. Polarization measurements

In Fig. 2 below are presented the polarization curves in the absence and in the presence of inhibitory Schiff bases at increasing concentrations, in 1M HCl medium at 35 °C.

Inhibitory efficacy is defined as follows:

$$E\% = \frac{i_{corr} - i'_{corr}}{i_{corr}} \times 100$$

where  $i_{corr}$  and  $i'_{corr}$  are the corrosion current density values of the steel determined by extrapolation of the Tafel cathode lines, after immersion in an acid medium respectively without and with the addition of the inhibitor.

Corrosion current density ( $i_{corr}$ ), corrosion potential ( $E_{corr}$ ), cathode and anode Tafel slopes ( $\beta_c$  and  $\beta_a$ ) and inhibition effi-

ciency  $E$  (%) for different concentrations of Schiff bases in 1M HCl medium are reported in Table 3.

Analysis of the data shown in Table 3, clearly shows that the corrosion current densities ( $i_{corr}$ ) decrease with increasing the concentration of ligand inhibitors, and that the inhibitory efficiency  $E$ (%) increases with increasing inhibitor concentration to reach a maximum of **97% at  $10^{-3}$  M** from  $IMP_1$ . This confirms the inhibitory nature of  $IMP_1$  obtained previously using mass loss measurements.

The addition of ligands to the corrosive medium causes a modification of the values of the Tafel slopes, indicating that both the anodic and cathodic reactions are affected, if the corrosion potential in the presence of the inhibitor does not shift by a value greater than 85 mV compared to white, the inhibitor can be considered as a mixed inhibitor. In our case, the variation of the potential does not exceed 70 mV. This result leads us to say that the ligands tested are inhibitors of the mixed type.

The cathodic polarization curves are in the form of straight lines indicating that the hydrogen reduction reaction on the surface of the steel takes place according to a pure activation mechanism.

Table 3

Potentiodynamic electrochemical parameters for the corrosion of mild steel in 1M HCl solution in the absence and presence of the investigated inhibitors at 308 K.

	Conc.(mol/l)	$E_{corr}$ (mVvs.CSE)	$i_{corr}$ (mA/cm <sup>2</sup> )	$\beta_c$ (mV)	$\beta_a$ (mV)	Efficiency(%)
Blank	1	-454.0	1.9477	-182.9	151.8	-
$IMP_1$	$10^{-3}$	-430.5	0.048	-124.7	72.4	97
	$5.10^{-4}$	-408.1	0.1471	-299.7	68.9	92
	$10^{-4}$	-447	0.3051	-236.9	80.1	84
	$5.10^{-5}$	-446.5	0.3445	-236.9	96.4	82
	$10^{-5}$	-470.1	0.8278	-221.8	146.7	57
$IMP_2$	$10^{-3}$	-483.8	0.1523	-139.8	91.5	92
	$5.10^{-4}$	-497.4	0.2068	-148.7	100.8	89
	$10^{-4}$	-488.8	0.5425	-184.6	115	72
	$5.10^{-5}$	-502.4	0.8494	-167.8	84.3	56
	$10^{-5}$	-494.4	1.3892	-191.2	96.5	28
$IMP_3$	$10^{-3}$	-480.8	0.5145	-218.4	114	76
	$5.10^{-4}$	-474.9	0.4562	-156.1	96.4	73
	$10^{-4}$	-473.1	1.1127	-209.9	107.2	42
	$5.10^{-5}$	-473	1.3248	-112.7	101.4	32
	$10^{-5}$	-463.9	1.5685	-179.6	114.5	19

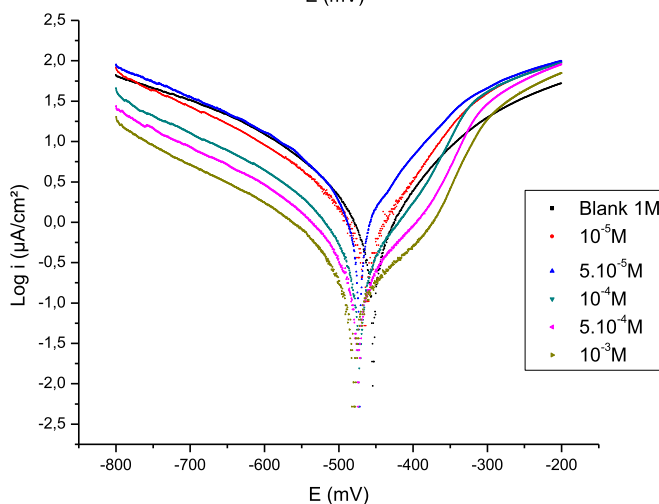
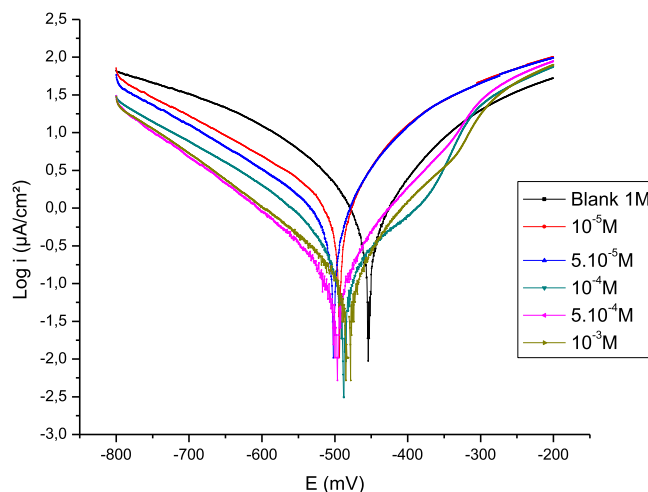
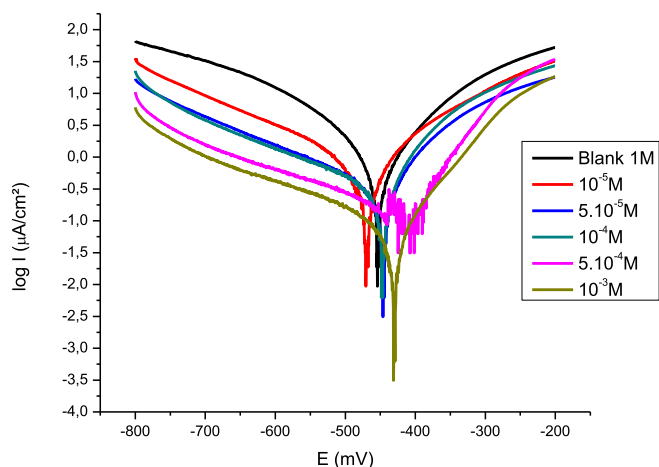


**Fig. 2.** Tafel polarization curves for mild steel obtained at 308 K in 1M HCl solution containing different concentrations of IMP<sub>1-3</sub>.

The Schiff bases compound proved to be the best inhibitor of this series with an efficiency reached 95% at a concentration of  $10^{-3}$ M.

### 3.2.2. Electrochemical impedance spectroscopy

The results obtained by the stationary electrochemical method show a satisfactory agreement with the previous methods. The order in which the efficiencies of the inhibitors are classified is always followed.

**Table 4**

Impedance parameters and inhibition efficiency for mild steel in 1.0 M HCl solutions containing different concentrations of IMP<sub>1</sub>, IMP<sub>2</sub> and IMP<sub>3</sub>.

ProdCode	Conc.(mol/l)	Rt( $\Omega$ .cm <sup>2</sup> )	C <sub>dl</sub> ( $\mu$ F.cm <sup>-2</sup> )	Efficiency(%)
Blank	1	20.7	191.7	-
IMP1	$10^{-3}$	723.4	34.8	97
	$5.10^{-4}$	521.5	38.5	96
	$10^{-4}$	98.6	80.6	78
	$5.10^{-5}$	80.2	99.1	74
	$10^{-5}$	42.7	186.4	51
	$5.10^{-4}$	159.4	65.2	87
IMP2	$10^{-3}$	133.9	77.6	84
	$10^{-4}$	105.8	98.2	80
	$5.10^{-5}$	60.01	106.1	65
	$10^{-5}$	32.97	150.9	37
	$10^{-3}$	103.4	76.9	80
	$5.10^{-4}$	93.26	85.3	77
IMP3	$10^{-4}$	45.95	109.5	54
	$5.10^{-5}$	32.14	123.8	35
	$10^{-5}$	26.72	148.9	22

The corresponding values of Rt and E (%) of steel in 1 M HCl in the absence and presence of IMP<sub>1</sub>, IMP<sub>2</sub> and IMP<sub>3</sub> are also given in Table 4.

The response of the impedance of the steel in the acid solution changed significantly after the addition of the three ligands and the impedance increased with increasing the content of the concentration of each inhibitor. In fact, the decrease in C<sub>dl</sub> values is due to the adsorption of imine components on the metal surface leading to the formation of a film which limits the corrosive effect of the acid solution.

We also note an increase in the corrosion inhibition efficiency due to the increase in Rct values with the concentration of the inhibitor which reaches 97% at  $10^{-3}$ M.

The results of electrochemical impedance spectroscopy agree with the other techniques.

### 3.3. Temperature effect

The temperature of the corrosive medium is a factor which can modify the inhibitory efficiency of an inhibitor and the metal-inhibitor interaction, as it can also provide information on the mechanism of action of the inhibitor (chemisorption or physisorption) and on the activation energies of the corrosion process. Given the importance of this factor, we have carried out mass loss tests for steel in 1M HCl acid without and with the addition of inhibitors, in a temperature range between 35 and 65 °C. This for an immersion time of one hour and at a concentration of  $10^{-3}$ M, a concentration for which the inhibitory efficiency of inhibitor reaches the maximum value at temperature 35 °C. We chose the gravimetric method since it best reflects the phenomenon of corrosion as it is in the real state.

The values of the corrosion rates and the inhibitory efficacy of the inhibitor, as a function of temperature, are given in Table 5.

The variation in the logarithm of the corrosion rate  $W_{\text{corr}}$  as a function of the inverse of the absolute temperature is recorded in the figure. The curves obtained are in the form of straight lines, so they obey the Arrhenius relation. The activation energies are therefore determined by the following relationship:

$$\ln(W) = \ln(A) - \frac{E_a}{RT}$$

where  $E_a$  represents the apparent activation energy, R the gas constant, T the absolute temperature, A is a pre-exponential factor, and W the corrosion rate obtained from the mass loss method (Figs. 3 and 4).

The apparent activation energy was determined from the slopes of  $\ln(W_{\text{corr}})$  as a function of  $(1000/T)$  shown in the Fig. 5.

**Table 5**  
the inhibitory efficiency and the corrosion rates in the absence and in the presence of inhibitors at different temperatures (K).

Compound	Temperature(K)	Concentration(Mol/l)	Corrosion rate(mg/cm <sup>2</sup> .h)	Efficiency(%)
HCl	313	1	2.603	-
	323	1	3.758	-
	333	1	4.156	-
	343	1	5.836	-
IMP <sub>1</sub>	313	10 <sup>-3</sup>	0.357	86
	323	10 <sup>-3</sup>	1.001	73
	333	10 <sup>-3</sup>	1.539	62
	343	10 <sup>-3</sup>	3.693	36
IMP <sub>2</sub>	313	10 <sup>-3</sup>	0.436	83
	323	10 <sup>-3</sup>	1.136	69
	333	10 <sup>-3</sup>	1.786	57
	343	10 <sup>-3</sup>	3.864	33
IMP <sub>3</sub>	313	10 <sup>-3</sup>	0.687	73
	323	10 <sup>-3</sup>	1.785	52
	333	10 <sup>-3</sup>	2.498	39
	343	10 <sup>-3</sup>	4.65	20

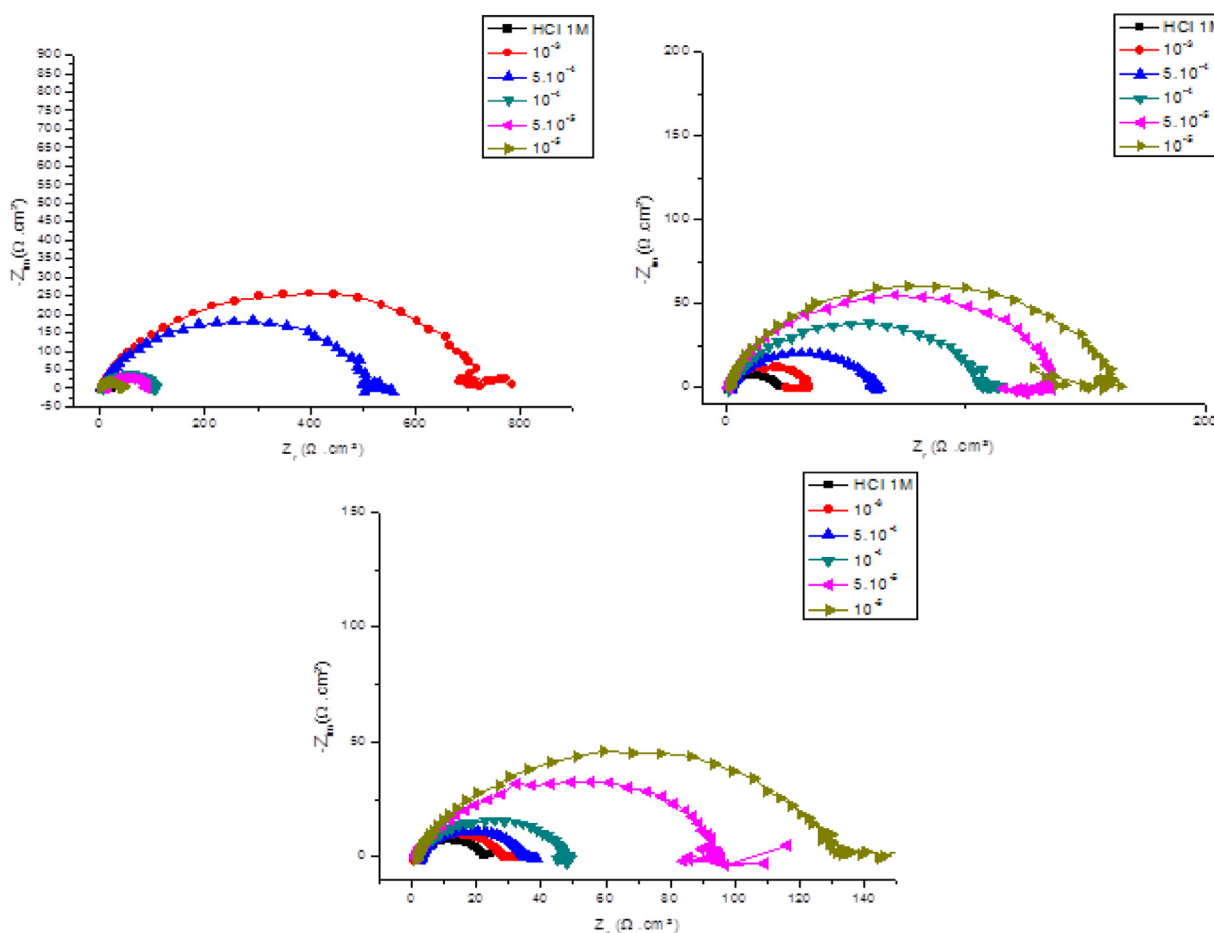


**Fig. 3.** Nyquist plot for mild steel in 1.0 M HCl solution in absence and presence of IMP<sub>1</sub>, IMP<sub>2</sub> and IMP<sub>3</sub>.

The Figure below gives the variation of Ln (W/T) as a function of the inverse of the absolute temperature in the form of lines with a slope of ((-ΔH<sub>R</sub><sup>0</sup>)/R) and the extrapolation of these lines gives the values of n (R/Nh + ΔS<sub>a</sub><sup>0</sup>/R) from which the values of ΔH<sub>a</sub><sup>0</sup> and ΔS<sub>a</sub><sup>0</sup> are calculated (Table 6).

$$\ln\left(\frac{W}{T}\right) = \left[ \ln\left(\frac{R}{Nh}\right) + \left(\frac{\Delta S_a^0}{R}\right) \right] - \frac{\Delta H_a^0}{RT}$$

The results in Table 6 show that:

- The thermodynamic parameters (ΔH<sub>a</sub><sup>0</sup>, ΔS<sub>a</sub><sup>0</sup>) of the reaction for dissolving steel in 1M HCl in the presence of the imidazole compound are higher than those of the solution without inhibitor.
- The entropy ΔS<sub>a</sub><sup>0</sup> is greater in the absence of inhibitory ligands, and this reflects a reduction in disorder during the transformation of the reagents into an iron-activated molecule complex in the solution [43,44].
- The comparison of the activation energies obtained in the presence and absence of the inhibitor makes it possible to know

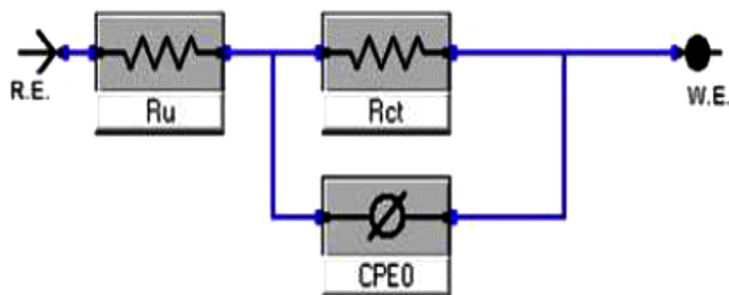


Fig. 4. Electrical equivalent circuit model used for the modeling metal/solution.

**Table 6**  
Activation parameters of mild steel in 1M HCl medium without and with the addition of IMP<sub>1-3</sub> compounds at 10<sup>-3</sup>M.

Compounds	C	E <sub>a</sub> (kJ mol <sup>-1</sup> )	ΔH <sub>a</sub> <sup>0</sup> (kJ mol <sup>-1</sup> )	ΔS <sub>a</sub> <sup>0</sup> (kJ mol <sup>-1</sup> )	E <sub>a</sub> <sup>0</sup> - ΔH <sub>a</sub> <sup>0</sup>
HCl	1	22.52	19.80	173.89	2.72
IMP <sub>1</sub>	10 <sup>-3</sup>	66.45	63.73	49.68	2.72
IMP <sub>2</sub>	10 <sup>-3</sup>	62.52	59.80	60.58	2.72
IMP <sub>3</sub>	10 <sup>-3</sup>	54.36	51.63	82.55	2.72

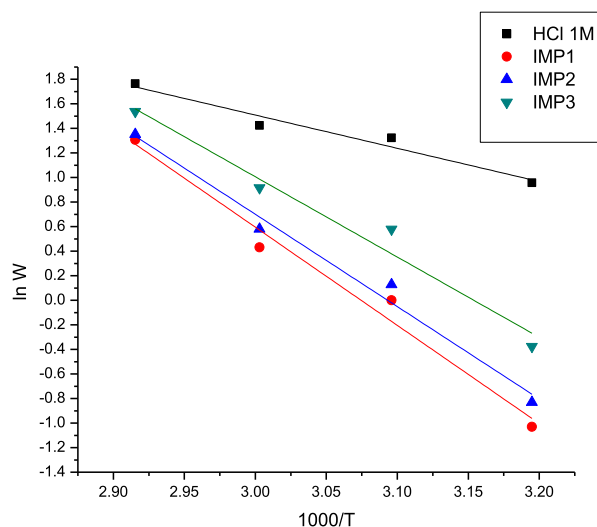


Fig. 5. Arrhenius lines calculated from the mass losses of steel in 1M HCl without and with 10<sup>-3</sup>M inhibitors.

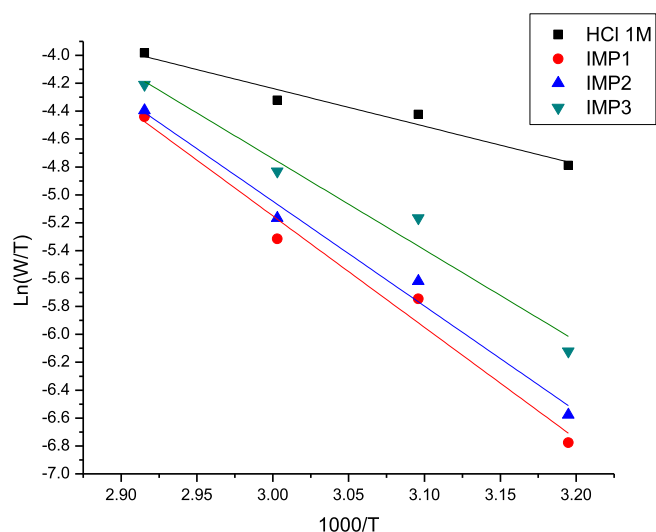


Fig. 6. Arrhenius plots from the mass losses of mild steel in the presence and absence of IMP inhibitors.

the type of adsorption. The activation energy in the presence of ligands is greater than that obtained in the acid alone. It can be concluded that the inhibitor studied is adsorbed on the surface by forming electrostatic bonds (physisorption).

- The positive sign of enthalpy  $\Delta H_a^0$  reflects the endothermic nature of the steel dissolution process.
- We note that the activation energy  $E_a$  and the activation enthalpy  $\Delta H_a^0$  vary in the same way with the inhibitor concentration (Table 6), verifying the thermodynamic relationship between  $E_a$  and  $\Delta H_a^0$  [45]:

$$E_a - \Delta H_a^0 = RT = \text{cste}$$

### 3.4. Quantum chemical calculation

Quantum chemical approaches were used to explain the molecular level behavior and electronic properties of IMP compounds whose corrosion inhibition efficiency was determined experimentally. For this purpose, IMP<sub>1-3</sub> compounds were examined using B3LYP and M062X methods and 6-31G(d), 6-31++G(d), LANL2DZ

and SDD basis sets using Density Function Theory (DFT) approach and the values of the relevant parameters for IMP<sub>1</sub>, IMP<sub>2</sub> and IMP<sub>3</sub> are listed in Tables 5–7 respectively.

In Tables 5–7, when the calculated quantum chemical parameters were examined, the most compatible calculation level with the experimental data was determined as B3LYP/6-31++G(d, p). Therefore, theoretical comments were interpreted taking into account the B3LYP/6-31++G(d, p) calculation level.  $E_{\text{HOMO}}$  is a parameter related to the molecule's ability to donate electrons. The tendency of the electron transfers of the compounds studied at the molecular level to the low empty molecular orbital of the appropriate acceptor molecule can be compared. Thus, with the increased energy of HOMO, the corrosion inhibition efficiency of the tapped molecule increases.

$E_{\text{LUMO}}$  represents the ability of a molecule to accept electrons and is a measure of the molecule's ability to bind to the metal surface in corrosion studies. The molecule with low  $E_{\text{LUMO}}$  value exhibits high corrosion inhibition properties. The difference between the LUMO energy and the HOMO energy is called the energy gap



**Table 7**  
The calculated quantum chemical descriptors for the IMP<sub>1</sub>.

Method	B3LYP				M062X			
	6-31G(d)	6-31++G(d)	LANL2DZ	SDD	6-31G(d)	6-31++G(d)	LANL2DZ	SDD
$E_{\text{HOMO}}$ (eV)	-4,543	-4,865	-4,848	-6,972	5,770	-6,026	-6,021	-6,022
$E_{\text{LUMO}}$ (eV)	-1,318	-2,219	-1,655	-1,163	0,435	-0,806	-0,806	-0,806
$\Delta E$ (eV)	3,225	2,647	3,193	5,808	5,335	5,220	5,216	5,216
$\eta$ (eV)	1,613	1,323	1,597	2,904	2,667	2,610	2,608	2,608
$\sigma$ (eV <sup>-1</sup> )	0,620	0,756	0,626	0,344	0,375	0,383	0,384	0,384
$\chi$ (eV)	2,931	3,542	3,252	4,068	3,103	3,416	3,414	3,414
$\mu$ (eV <sup>-1</sup> )	-2,931	-3,542	-3,252	-4,068	-3,103	-3,416	-3,414	-3,414
$\omega$	2,663	4,740	3,312	2,848	1,804	2,235	2,234	2,235
$\varepsilon$	0,376	0,211	0,302	0,351	0,554	0,448	0,448	0,448
$\omega^+$	0,993	1,705	1,242	0,981	0,542	0,739	0,739	0,739
$\omega^-$	4,330	6,676	5,137	5,245	3,689	4,269	4,267	4,268
$\Delta N$	0,586	0,483	0,491	0,130	0,322	0,269	0,270	0,270
$\alpha$	266,640	305,060	276,940	277,400	243,770	275,130	255,910	256,130

**Table 8**  
The calculated quantum chemical descriptors for the IMP<sub>2</sub>.

Method	B3LYP				M062X			
	6-31G(d)	6-31++G(d)	LANL2DZ	SDD	6-31G(d)	6-31++G(d)	LANL2DZ	SDD
$E_{\text{HOMO}}$ (eV)	-4,796	-5,068	-5,124	-7,004	-0,435	-6,178	-6,276	-6,270
$E_{\text{LUMO}}$ (eV)	-1,676	-2,019	-2,047	-0,640	-0,857	-1,179	-1,219	-1,208
$\Delta E$ (eV)	3,120	3,049	3,078	6,364	5,098	5,000	5,057	5,062
$\eta$ (eV)	1,560	1,525	1,539	3,182	2,549	2,500	2,529	2,531
$\sigma$ (eV <sup>-1</sup> )	0,641	0,656	0,650	0,314	0,392	0,400	0,396	0,395
$\chi$ (eV)	3,236	3,543	3,585	3,822	3,407	3,679	3,747	3,739
$\mu$ (eV <sup>-1</sup> )	-3,236	-3,543	-3,585	-3,822	-3,407	-3,679	-3,747	-3,739
$\omega$	3,357	4,117	4,177	2,295	2,276	2,706	2,777	2,761
$\varepsilon$	0,298	0,243	0,239	0,436	0,439	0,370	0,360	0,362
$\omega^+$	1,258	1,526	1,548	0,711	0,763	0,955	0,982	0,976
$\omega^-$	5,170	6,079	6,162	4,604	4,298	4,858	4,967	4,947
$\Delta N$	0,508	0,419	0,401	0,157	0,277	0,228	0,212	0,214
$\alpha$	279,200	317,080	287,210	277,400	256,480	288,725	265,530	265,540

**Table 9**  
The calculated quantum chemical descriptors for the IMP<sub>3</sub>.

Method	B3LYP				M062X			
	6-31G(d)	6-31++G(d)	LANL2DZ	SDD	6-31G(d)	6-31++G(d)	LANL2DZ	SDD
$E_{\text{HOMO}}$ (eV)	-5,321	-5,628	-6,558	-6,541	-6,562	-6,639	-6,817	-6,813
$E_{\text{LUMO}}$ (eV)	-2,762	-1,576	-2,791	-2,655	-2,237	-2,234	-2,524	-2,512
$\Delta E$ (eV)	2,559	4,052	3,767	3,885	4,326	4,405	4,292	4,301
$\eta$ (eV)	1,280	2,026	1,884	1,943	2,163	2,203	2,146	2,151
$\sigma$ (eV <sup>-1</sup> )	0,782	0,494	0,531	0,515	0,462	0,454	0,466	0,465
$\chi$ (eV)	4,041	3,602	4,674	4,598	4,399	4,436	4,670	4,662
$\mu$ (eV <sup>-1</sup> )	-4,041	-3,602	-4,674	-4,598	-4,399	-4,436	-4,670	-4,662
$\omega$	6,382	3,201	5,800	5,441	4,474	4,467	5,082	5,054
$\varepsilon$	0,157	0,312	0,172	0,184	0,224	0,224	0,197	0,198
$\omega^+$	2,175	1,191	2,125	2,011	1,678	1,675	1,898	1,889
$\omega^-$	8,562	5,255	8,373	7,983	6,944	6,961	7,685	7,654
$\Delta N$	0,304	0,301	0,039	0,057	0,097	0,087	0,035	0,037
$\alpha$	333,980	363,820	314,960	305,140	298,960	300,570	316,670	316,420

$\Delta E$ . It represents the predisposition of the inhibitor molecule to metal surface adsorption. As the E value decreases, the corrosion inhibition efficiency increases.

So far, the order of the inhibition efficiency of the molecules obtained from the theoretical results is as follows  $\text{IMP}_1 > \text{IMP}_2 > \text{IMP}_3$ .

One of the applications of theoretical foundations in corrosion studies is the HSAB (hard-soft-acid-base) approach. According to this approach, hard acids prefer to complex with hard bases and soft acids prefer to complex with soft bases. In other words, metallic piles prefer to form complexes with soft chemical species. Thus, the examined chemical type in determining the corrosion inhibition efficiency should have low hardness and high softness (Tables 8 and 9).

According to the application of the Koopmans theorem, electronegativity and chemical potential, the opposite of each other, can be interpreted for the corrosion inhibition efficacy with the same approach. In accordance with Sanderson's principle of electronegativity equalization, the low difference of electronegativity between the metal and the inhibitor should increase the inhibitor reactivity. In chemical potential values, it is expected to be the opposite of this situation. As a result, inhibition efficiency increases with low electronegativity and high chemical potential.

Electron transfer fractions, which are the application of Pearson method, are also used quite frequently in determining the corrosion inhibition effectiveness. The  $\chi_{\text{Fe}}$  and  $\eta_{\text{Fe}}$  parameters for iron in this parameter are 4.82 and 0 eV, respectively. If  $\Delta N > 0$ , the electrons of the molecule cover the relevant metal surface. If the

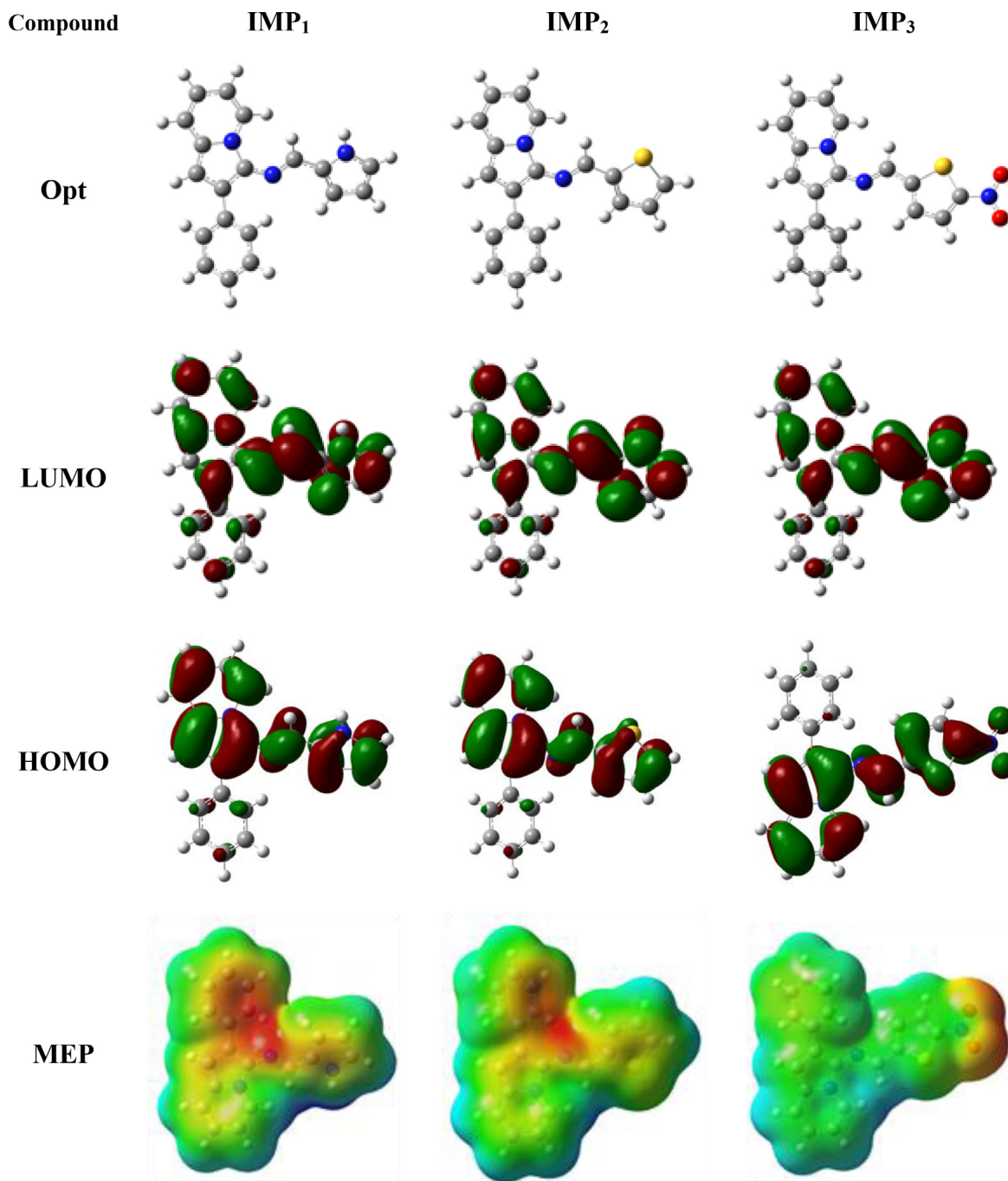


Fig. 7. Optimized structures, HOMOs, LUMOs and MEP maps for IMP<sub>1-3</sub>.

$\Delta N$  value of the molecule is less than 3.6, the inhibition efficiency is high. Because electron donation increases on the metal surface. This shows that the inhibitory molecule gives electrons to the empty d orbital of the metal and the inhibitor interacts with the metallic surface.

In recent years, two new parameters have received considerable attention in quantum chemical studies. One of these,  $\omega^-$ , represents electron donation power to chemical species. The other is  $\omega^+$ , representing electron acceptance power. Among these parameters, increasing the value of  $\omega^-$  and decreasing the value of  $\omega^+$  is a criterion in determining the order of corrosion inhibition efficiency of chemical species.

In addition to all this, the parameter which is a function of the dipole moment is polarizability. Polarization is a linear representation of electron density in the presence of an electric field. As the polarizability increases, the corrosive effect of the molecule increases. However, the results obtained in this section tended to be the opposite of experimental results. The order of inhibition efficiency obtained at B3LYP/6-31++G(d) level for the examined compounds gives us  $IMP_1 > IMP_2 > IMP_3$ . This is quite compatible with experimental results (Fig. 6).

Moreover, optimized structures, frontier molecular orbitals and molecular electrostatic potential (MEP) maps obtained at the most appropriate computational level for the compounds are given in Fig. 7

When HOMO molecular orbitals are examined, it is noteworthy that the electron density is in the molecular plane. Also, HOMO's electrons are on the aromatic ring. There is electron delocalization in **IMP<sub>1-3</sub>** compounds and electrons are dispersed along the chemical surface. In the electron distribution of LUMO molecular orbitals, the only striking point is that the electron density of imp3 compounds is on the phenyl ring. In the MEP maps, it is seen that the electron attracting region in the imp1 compound is more than other compounds. It is also worth noting that in the **IMP<sub>3</sub>** compound, the electrophilic region is dense on the oxygen atom.

#### 4. Conclusion

Three new Imidazopyridine derivatives were synthesized and identified by <sup>1</sup>H and <sup>13</sup>C NMR. The inhibitors studied in this work are good inhibitors of corrosion of steel in hydrochloric acid (1M) medium, and the inhibitory efficacy calculated by the methods used are in good agreement.

The addition of these inhibitors acts only by reducing the cathodic surface without changing the mechanism of the cathodic reaction.

The adsorption of ligands synthesized on the surface follows the Langmuir isotherm model.

Examination of the temperature on the corrosion resistance reveals that increasing the temperature in the range 35–65 °C decreases the inhibitory efficiency.

The variation in activation energy in the presence of these inhibitors can be attributed to the physisorption of the inhibitor on the surface of the steel.

#### Declaration of Competing Interest

The authors declare that they have no known competing financial interests or personal relationships that could have appeared to influence the work reported in this paper.

#### CRediT authorship contribution statement

**Abdelmalik EL AATIAOUI:** Conceptualization, Writing - original draft, Methodology, Formal analysis. **Mohammed KOUDAD:** Methodology, Formal analysis. **Tarik CHELFI:** Writing - review & editing, Methodology, Conceptualization, Formal analysis. **Sultan ERKAN:** Data curation, Formal analysis, Software. **Mohamed AZ-ZOUZI:** Methodology, Formal analysis. **Abdelouahad AOUNITI:** Project administration, Resources, Methodology, Formal analysis. **Kaya SAVAŞ:** Data curation, Formal analysis, Software. **Mohammed KADDOURI:** Methodology, Formal analysis. **Noureddine BENCHAT:** Project administration, Resources, Methodology, Formal analysis. **Adyl OUSSAID:** Project administration, Resources, Methodology, Formal analysis.

#### Acknowledgements

The authors are grateful to the National Center for Scientific and Technical Research (CNRST) for funding this work and would like to extend their sincere appreciation to VILLAPHARMA RESEARCH SL for supporting this Research group and spectroscopic analysis, and Prof. Brahim AMANCHAR for reviewing all the text in order to correct the language mistakes.

#### References

- [1] A. Ghazoui, R. Saddik, B. Hammouti, A. Zarrouk, N. Benchat, M. Guenbour, S.S. Al-Deyab, I. Warad, Inhibitive effect of imidazopyridine derivative towards corrosion of C38 steel in hydrochloric acid solution, *Res. Chem. Intermed.* (2013), doi:10.1007/s11164-012-0763-y.
- [2] R. Salim, E. Ech Chihbi, H. Oudda, Y. ELAoufir, F. El-Hajjaji, A. Elaataoui, A. Ousaid, B. Hammouti, H. Elmsellem, M. Taleb, The inhibition effect of imidazopyridine derivatives on C38 steel in hydrochloric acid solution, *Der Pharma Chem.* 8 (3) (2016) 200–213.
- [3] A. Anejjar, R. Salghi, A. Zarrouk, H. Zarrok, O. Benali, B. Hammouti, S.S. Al-Deyab, N.E. Benchat, R. Saddik, Investigation of inhibition by 6-bromo-3-nitroso-2-phenylimidazo[1,2- $\alpha$ ]pyridine of the corrosion of C38 steel in 1 M HCl, *Res. Chem. Intermed.* 41 (2015) 913–925, doi:10.1007/s11164-013-1244-7.
- [4] A. Ghazoui, R. Saddik, N. Benchat, B. Hammouti, M. Guenbour, A. Zarrouk, M. Ramdani, The role of 3-amino-2-phenylimidazo[1,2- $\alpha$ ]pyridine as corrosion inhibitor for C38 steel in 1M HCl, *Der Pharma Chem.* 4 (1) (2012) 352–364.
- [5] D. Ben Hmamou, R. Salghi, A. Zarrouk, H. Zarrok, B. Hammouti, S.S. Al-Deyab, A. El Assyry, N. Benchat, M. Bouachrine, Electrochemical and gravimetric evaluation of 7-methyl-2-phenylimidazo[1,2- $\alpha$ ]pyridine of carbon steel corrosion in phosphoric acid solution, *Int. J. Electrochem. Sci.* 8 (2013) 11526–11545.
- [6] G. Puerstinger, J. Paeshuysse, E. De Clercq, J. Neyts, Antiviral 2, 5-disubstituted imidazo[4,5-c]pyridines: from anti-pestivirus to anti-hepatitis C virus activity, *Bioorganic Med. Chem. Lett.* (2007), doi:10.1016/j.bmcl.2006.10.039.
- [7] C. Hamdouchi, B. Zhong, J. Mendoza, E. Collins, C. Jaramillo, J.E. De Diego, D. Robertson, C.D. Spencer, B.D. Anderson, S.A. Watkins, F. Zhang, H.B. Brooks, Structure-based design of a new class of highly selective aminoimidazo[1,2- $\alpha$ ]pyridine-based inhibitors of cyclin dependent kinases, *Bioorg. Med. Chem. Lett.* (2005), doi:10.1016/j.bmcl.2005.01.052.
- [8] K.S. Gudmundsson, B.A. Johns, Imidazo[1,2- $\alpha$ ]pyridines with potent activity against herpesviruses, *Bioorg. Med. Chem. Lett.* (2007), doi:10.1016/j.bmcl.2007.02.079.
- [9] D.-J. Zhu, J.-X. Chen, M.-C. Liu, J.-C. Ding, H.-Y. Wu, Catalyst: and solvent-free synthesis of imidazo[1,2- $\alpha$ ]pyridines, *J. Braz. Chem. Soc.* 20 (2009) 482–487.
- [10] W.W. Paudler, D.E. Dunham, Ten- $\pi$ -electron nitrogen heterocyclic compounds VI: NMR spectra, HMO calculations and bromination of some diazaindenes, *J. Heterocycl. Chem.* (1965), doi:10.1002/jhet.5570020417.
- [11] M. Behpour, S.M. Ghoreishi, N. Soltani, M. Salavati-Niasari, The inhibitive effect of some bis-N,S-bidentate Schiff bases on corrosion behaviour of 304 stainless steel in hydrochloric acid solution, *Corros. Sci.* (2009), doi:10.1016/j.corsci.2009.02.011.
- [12] H. Ju, Z.P. Kai, Y. Li, Aminic nitrogen-bearing polydentate Schiff base compounds as corrosion inhibitors for iron in acidic media: a quantum chemical calculation, *Corros. Sci.* (2008), doi:10.1016/j.corsci.2007.10.009.
- [13] H.D. Leçe, K.C. Emregül, O. Atakol, Difference in the inhibitive effect of some Schiff base compounds containing oxygen, nitrogen and sulfur donors, *Corros. Sci.* (2008), doi:10.1016/j.corsci.2008.01.014.
- [14] R.A. Prabhu, T.V. Venkatesha, A.V. Shanbhag, G.M. Kulkarni, R.G. Kalkhambkar, Inhibition effects of some Schiff's bases on the corrosion of mild steel in hydrochloric acid solution, *Corros. Sci.* (2008), doi:10.1016/j.corsci.2008.09.009.
- [15] C. Küstü, K.C. Emregül, O. Atakol, Schiff bases of increasing complexity as mild steel corrosion inhibitors in 2 M HCl, *Corros. Sci.* (2007), doi:10.1016/j.corsci.2007.02.002.
- [16] E. McCafferty, N. Hackerman, Closure to "discussion of 'kinetics of iron corrosion in concentrated acidic chloride solutions', *J. Electrochem. Soc.* 119 (8) (1973) 999–1009, doi:10.1149/1.2403559.
- [17] M. Elayyachy, A. El Idrissi, B. Hammouti, New thio-compounds as corrosion inhibitor for steel in 1 M HCl, *Corros. Sci.* (2006), doi:10.1016/j.corsci.2005.09.016.
- [18] A.M. Abdel-Gaber, M.S. Masoud, E.A. Khalil, E.E. Shehata, Electrochemical study on the effect of Schiff base and its cobalt complex on the acid corrosion of steel, *Corros. Sci.* (2009), doi:10.1016/j.corsci.2009.08.025.
- [19] W. Zhang, H.J. Li, M. Wang, L.J. Wang, A.H. Zhang, Y.C. Wu, Highly effective inhibition of mild steel corrosion in HCl solution by using pyrido[1,2- $\alpha$ ]benzimidazoles, *New J. Chem.* (2019), doi:10.1039/C8NJ04028A.
- [20] K.C. Emregül, O. Atakol, Corrosion inhibition of mild steel with Schiff base compounds in 1 M HCl, *Mater. Chem. Phys.* (2003), doi:10.1016/S0254-0584(03)00204-9.
- [21] S. Bilgiç, N. Çaliskan, Effect of N-(1-toluidine) salicylaldehyde on the corrosion of austenitic chromium-nickel steel, *Appl. Surf. Sci.* (1999), doi:10.1016/S0169-4332(99)00308-6.
- [22] M. Hosseini, S.F.L. Mertens, M. Ghorbani, M.R. Arshadi, Asymmetrical Schiff bases as inhibitors of mild steel corrosion in sulphuric acid media, *Mater. Chem. Phys.* (2003), doi:10.1016/S0254-0584(02)00390-5.
- [23] M. Yadav, D. Behera, R.R. Sinha, P.N. Yadav, Experimental and quantum studies on adsorption and corrosion inhibition effect on mild steel in hydrochloric acid by thiophene derivatives, *Acta Metall. Sin. (Engl. Lett.)* (2014), doi:10.1007/s40195-013-0012-4.
- [24] M.N. Desai, M.B. Desai, C.B. Shah, S.M. Desai, Schiff bases as corrosion inhibitors for mild steel in hydrochloric acid solutions, *Corros. Sci.* (1986), doi:10.1016/0010-938X(86)90066-1.
- [25] H. Ashassi-Sorkhabi, B. Shaabani, D. Seifzadeh, Corrosion inhibition of mild steel by some Schiff base compounds in hydrochloric acid, *Appl. Surf. Sci.* (2005), doi:10.1016/j.apsusc.2004.05.143.
- [26] N.Z. Nor Hashim, K. Kassim, B.M. Yamin, N-[(E)-4-Chloro-benzyl-idene]-N'-phenyl-benzene-1,4-diamine, *Acta Crystallogr. Sect. E* (2010), doi:10.1107/S160053681002742X.
- [27] V.V. Torres, V.A. Rayol, M. Magalhães, G.M. Viana, L.C.S. Aguiar, S.P. Machado, H. Orofino, E. D'Elia, Study of thioureas derivatives synthesized from a green route as corrosion inhibitors for mild steel in HCl solution, *Corros. Sci.* (2014), doi:10.1016/j.corsci.2013.10.032.

- [28] D. Daoud, T. Douadi, S. Issaadi, S. Chafaa, Adsorption and corrosion inhibition of new synthesized thiophene Schiff base on mild steel X52 in HCl and H<sub>2</sub>SO<sub>4</sub> solutions, *Corros. Sci.* (2014), doi:[10.1016/j.corsci.2013.10.025](https://doi.org/10.1016/j.corsci.2013.10.025).
- [29] N.Z.N. Hashim, K. Kassim, The effect of temperature on mild steel corrosion in 1 M HCl by Schiff bases, *Malays. J. Anal. Sci.* 18 (1) (2014) 28–36.
- [30] A. Elaataoui, F. Elkalai, N. Benchat, M. Saadi, L. El Ammari, (*E*)-2-Phenyl-N-(thio-phen-2-yl-methyl-ide)imidazo[1,2-*a*]pyridin-3-amine, *IUCrData* (2016), doi:[10.1107/s2414314616007239](https://doi.org/10.1107/s2414314616007239).
- [31] A. Frumkin, Die Kapillarkurve der höheren Fettsäuren und die Zustandsgleichung der Oberflächenschicht, *Zeitschrift Für Phys. Chemie.* 116U (1925) 466–484, doi:[10.1515/zpch-1925-11629](https://doi.org/10.1515/zpch-1925-11629).
- [32] J. Dennington, Roy; Keith, Todd; Millam, GaussView 5, Semichem Inc., Shawnee Mission, KS, 2009.
- [33] M.J.G. Frisch, W. Trucks, H.B. Schlegel, G.E. Scuseria, M.A. Robb, J.R. Cheeseman, G. Scalmani, V. Barone, B. Mennucci, G.A. Petersson, H. Nakatsuji, M. Caricato, X. Li, H.P. Hratchian, A.F. Izmaylov, J. Bloino, G. Zheng, J.L. Sonnenberg, Gaussian 16 Rev. D.01 (2016) 111.
- [34] D. Tarkhov, A. Vasilyev, Academic Press, 2020, pp. 51–72, doi:[10.1016/B978-0-12-815651-3.00002-X](https://doi.org/10.1016/B978-0-12-815651-3.00002-X).
- [35] O. Fergachi, F. Benhiba, M. Rbaa, M. Ouakki, M. Galai, R. Touri, B. Lakhri, H. Oudda, M.E. Touhami, Corrosion inhibition of ordinary steel in 5.0 M HCl medium by benzimidazole derivatives: electrochemical, UV-visible spectrometry, and DFT calculations, *J. Bio-Tribo-Corros.* 5 (2019) 21, doi:[10.1007/s40735-018-0215-3](https://doi.org/10.1007/s40735-018-0215-3).
- [36] J. Haque, V. Srivastava, D.S. Chauhan, H. Lgaz, M.A. Quraishi, Microwave-induced synthesis of chitosan Schiff bases and their application as novel and green corrosion inhibitors: experimental and theoretical approach, *ACS Omega* 3 (2018) 5654–5668, doi:[10.1021/acsomega.8b00455](https://doi.org/10.1021/acsomega.8b00455).
- [37] F. El-Hajjaji, M. Messali, A. Aljuhani, M.R. Aouad, B. Hammouti, M.E. Belghiti, D.S. Chauhan, M.A. Quraishi, Pyridazinium-based ionic liquids as novel and green corrosion inhibitors of carbon steel in acid medium: Electrochemical and molecular dynamics simulation studies, *J. Mol. Liq.* 249 (2018), doi:[10.1016/j.molliq.2017.11.111](https://doi.org/10.1016/j.molliq.2017.11.111).
- [38] P. Singh, D.S. Chauhan, K. Srivastava, V. Srivastava, M.A. Quraishi, Expired atorvastatin drug as corrosion inhibitor for mild steel in hydrochloric acid solution, *Int. J. Ind. Chem.* 8 (2017) 363–372, doi:[10.1007/s40090-017-0120-5](https://doi.org/10.1007/s40090-017-0120-5).
- [39] P. Singh, V. Srivastava, M.A. Quraishi, Novel quinoline derivatives as green corrosion inhibitors for mild steel in acidic medium: electrochemical, SEM, AFM, and XPS studies, *J. Mol. Liq.* 216 (2016) 164–173, doi:[10.1016/j.molliq.2015.12.086](https://doi.org/10.1016/j.molliq.2015.12.086).
- [40] S. Issaadi, T. Douadi, A. Zouaoui, S. Chafaa, M.A. Khan, G. Bouet, Novel thiophene symmetrical Schiff base compounds as corrosion inhibitor for mild steel in acidic media, *Corros. Sci.* (2011), doi:[10.1016/j.corsci.2011.01.022](https://doi.org/10.1016/j.corsci.2011.01.022).
- [41] K.R. Ansari, M.A. Quraishi, A. Singh, Schiff's base of pyridyl substituted triazoles as new and effective corrosion inhibitors for mild steel in hydrochloric acid solution, *Corros. Sci.* 79 (2014), doi:[10.1016/j.corsci.2013.10.009](https://doi.org/10.1016/j.corsci.2013.10.009).
- [42] I. Jevremović, M. Singer, S. Nešić, V. Miskovic-Stanković, Inhibition properties of self-assembled corrosion inhibitor talloil diethylenetriamine imidazoline for mild steel corrosion in chloride solution saturated with carbon dioxide, *Corros. Sci.* (2013), doi:[10.1016/j.corsci.2013.08.012](https://doi.org/10.1016/j.corsci.2013.08.012).
- [43] M. Benabdellah, A. Ousslim, B. Hammouti, A. Elidrissi, A. Aouniti, A. Dafali, K. Bekkouch, M. Benkaddour, The effect of poly(vinyl caprolactone-co-vinyl pyridine) and poly(vinyl imidazol-co-vinyl pyridine) on the corrosion of steel in H<sub>3</sub>PO<sub>4</sub> media, *J. Appl. Electrochem.* (2007), doi:[10.1007/s10800-007-9317-1](https://doi.org/10.1007/s10800-007-9317-1).
- [44] S.S. Abd El-Rehim, M.A.M. Ibrahim, K.F. Khaled, 4-Aminoantipyrine as an inhibitor of mild steel corrosion in HCl solution, *J. Appl. Electrochem.* (1999), doi:[10.1023/A:1003450818083](https://doi.org/10.1023/A:1003450818083).
- [45] M. Elachouri, M.S. Hajji, M. Salem, S. Kertit, J. Aride, R. Coudert, E. Essassi, Some nonionic surfactants as inhibitors of the corrosion of iron in acid chloride solutions, *Corros.* (1996), doi:[10.5006/1.3292100](https://doi.org/10.5006/1.3292100).

NEW

The power of the Web of Science™ on your mobile device, wherever inspiration strikes.

Dismiss

Learn More

### Already have a manuscript?

Use our Manuscript Matcher to find the best relevant journals!

Find a Match

### Filters

Clear All

Web of Science Coverage

Open Access

Category

Country / Region

Language

Frequency

Journal Citation Reports

## Refine Your Search Results

JOURNAL OF MOLECULAR STRUCTURE

Search

Sort By: Relevancy

### Search Results

Found 948 results (Page 1)

Share These Results

### Exact Match Found

#### JOURNAL OF MOLECULAR STRUCTURE

Publisher: ELSEVIER , RADARWEG 29, AMSTERDAM, NETHERLANDS, 1043 NX

ISSN / eISSN: 0022-2860 / 1872-8014

Web of Science Core Collection: Science Citation Index Expanded

Additional Web of Science Indexes: Current Contents Physical, Chemical & Earth Sciences | Essential Science Indicators

Share This Journal

View profile page

### Other Possible Matches

#### NATURE STRUCTURAL & MOLECULAR BIOLOGY

Publisher: NATURE PORTFOLIO , HEIDELBERGER PLATZ 3, BERLIN, Germany, 14197

ISSN / eISSN: 1545-9993 / 1545-9985

Web of Science Core Collection: Science Citation Index Expanded

Additional Web of Science Indexes: Biological Abstracts | BIOSIS Previews | Current Contents Life Sciences | Essential Science Indicators

Share This Journal

View profile page

#### ALGORITHMS FOR MOLECULAR BIOLOGY

OPEN ACCESS

Publisher: BMC , CAMPUS, 4 CRINAN ST, LONDON, ENGLAND, N1 9XW

ISSN / eISSN: 1748-7188



# Web of Science



Search

Tools Searches and alerts Search History Marked List

## Results: 1

(from Web of Science Core Collection)

You searched for: TITLE: (Effect of hydrocarbon chain length for acid corrosion inhibition of mild steel by three 8-(n-bromo-R-alkoxy)quinoline derivatives: Experimental and theoretical investigations) ...[More](#)

Create an alert

## Refine Results

Search within results for...

### Publication Years

2021 (1)

Refine

### Web of Science Categories

CHEMISTRY PHYSICAL (1)

Refine

### Document Types

ARTICLE (1)

Refine

### Organizations-Enhanced

- CUMHURIYET UNIVERSITY (1)
- IBN TOFAIL UNIVERSITY OF KENITRA (1)
- IBN ZOHR UNIVERSITY OF AGADIR (1)
- MOHAMMED V UNIVERSITY IN RABAT (1)
- REG CTR EDUC TRAINING PROFESS CRMEF (1)

[more options / values...](#)

Refine

### Funding Agencies

### Authors

### Source Titles

[View all options](#)

For advanced refine options, use

[Analyze Results](#)

Sort by: Date Times Cited Usage Count Relevance More

1 of 1

Select Page Export... Add to Marked List

1. **Effect of hydrocarbon chain length for acid corrosion inhibition of mild steel by three 8-(n-bromo-R-alkoxy)quinoline derivatives: Experimental and theoretical investigations**

By: Tazouti, A.; Errahmany, N.; Rbaa, M.; et al.

JOURNAL OF MOLECULAR STRUCTURE Volume: 1244 Article Number: 130976 Published: NOV 15 2021

View Abstract

Select Page Export... Add to Marked List

Sort by: Date Times Cited Usage Count Relevance

Show: 10 per page

1 records matched your query of the 78,725,508 in the data limits you set

Analyze Results  
Create Citation Report

Times Cited: 1  
(from Web of Science Core Collection)

Usage Count

JOURNAL OF MOLECULAR STRUCTURE

Impact Factor  
**3.196** **2.618**  
2020 5 year

JCR® Category	Rank in Category	Quartile in Category
CHEMISTRY, PHYSICAL	<b>83 of 162</b>	<b>Q3</b>

Data from the 2020 edition of Journal Citation Reports

**Publisher**  
ELSEVIER, RADARWEG 29, 1043 NX AMSTERDAM, NETHERLANDS  
**ISSN:** 0022-2860  
**eISSN:** 1872-8014

**Research Domain**  
Chemistry

Close Window

Clarivate

Accelerating innovation